

## Research Article

# Experimental Study on Influence of Microexpansive Concrete Self-Stress on Performance of Steel Pipe Concrete

Xin Liu , Yu-Zhou Zheng , Qin Fang, Heng-Bo Xiang, and Hai-Chun Yan

State Key Laboratory of Disaster Prevention and Mitigation of Explosion and Impact, Army Engineering University of PLA, Nanjing, Jiangsu 210007, China

Correspondence should be addressed to Yu-Zhou Zheng; universe2009@126.com

Received 19 July 2021; Revised 26 October 2021; Accepted 26 November 2021; Published 7 December 2021

Academic Editor: Simon Laflamme

Copyright © 2021 Xin Liu et al. This is an open access article distributed under the Creative Commons Attribution License, which permits unrestricted use, distribution, and reproduction in any medium, provided the original work is properly cited.

To explore the influence of microexpansive concrete self-stress on the performance of steel pipe concrete, the expansion rate test of microexpansive concrete confined by steel tube was carried out with different expansion rates. Then, the mechanical properties of high-strength steel tube-confined microexpansive concrete (HSTCMC) short columns were conducted by the uniaxial compression test. The length-to-diameter ratio, the expansion rate of the microexpansive concrete, and the steel tube thickness were investigated in the study. Furthermore, the ABAQUS software was employed to analyze the microexpansive mechanism of the concrete, and it was verified by the uniaxial compression test. The test results show that the concrete possesses a remarkable volume expansion phenomenon, which was up to  $150 \mu\epsilon$  after four days of maintenance time. The mechanical properties of the HSTCMC short columns were greatly improved compared to the control RC pier. The yield and ultimate strength of the HSTCMC short columns can be enhanced to 8.9% and 14.6%, and with the content of expansive agent that increased from 8% to 12%. The finite element analysis results highlighted that the end constraint at the two ends has the biggest influence on the mechanical performance of the HSTCMC short columns, followed by the thickness of the steel tube and the content of the expansive agent. It should be noted that the self-stress of microexpansive concrete will be decreased with the increase in the length-to-diameter ratio, when the length-to-diameter ratio is less than four. Furthermore, the constraint effect of the circular steel tube on the microexpansive concrete is better than that of the rectangular section steel tube.

## 1. Introduction

In recent years, long-span high-rise building structures are emerging, and as the main load-bearing component, the mechanical performance of the pier column is particularly important. Due to the excellent mechanical properties of high strength, good durability, high stiffness, simple construction, and other advantages for the concrete-filled steel tube structure, the advantages of steel tube and concrete are fully utilized, and concrete can effectively delay the local buckling of steel tube, enhance the axial compressive strength of concrete, and improve the toughness of concrete-filled steel tube members. Therefore, it has been widely used and developed in the field of civil engineering structures. However, shrinkage and creep as the inherent properties of concrete will seriously reduce the compactness of concrete in

steel tube and influence the bonding performance between the steel tube and core concrete, especially in the large-volume concrete-filled steel tube structures. Fortunately, the microexpansive concrete with excellent expansion performance appeared, which can solve this problem well [1–6].

Many scholars both at home and abroad have carried out related research on microexpansive concrete-filled steel tube in the literature. Hu et al. [7] have studied the free curing and airtight curing of high-performance microexpansive concrete and found that the microstructure of microexpansive concrete can be effectively improved under the constraint conditions. Xu et al. [8, 9] have found that the self-stress of the concrete can significantly improve the uniaxial compression performance of the HSS-CFST, and the bearing capacity of the long columns ( $L/D > 4$ ) with microexpansive concrete can be improved by increasing the self-stress and

strength of microexpansive concrete. When the initial self-stress is 5 MPa, the ultimate bearing capacity of the steel tube self-stress concrete long columns is increased by 19%. Li et al. [10] have carried out axial compression tests on 36 concrete-filled steel tube columns, and the test results showed that the content of steel fiber and self-stress have an influence on the failure mode. Steel fiber and self-stress increase the ultimate load of CFST columns. Wang et al. [11] and other scholars have found that the effect of the self-stress for the concrete-filled steel tube specimen is a quadratic function distribution. Lu et al. [12, 13] found that the initial self-stress can significantly improve the bearing capacity of the steel fiber-reinforced microexpansive concrete short columns, the self-stress can significantly improve the bonding strength between the steel tube and concrete, and there is an optimal value of steel fiber content for improving the bond performance. He et al. [14] found that when the hoop coefficient is small, the radial deformation of steel tube reduces the constraint effect of steel tube on microexpansive concrete, and the effect of improving the bearing capacity of members is not obvious. Lu et al. [15] and Liu et al. [16, 17] have studied that the ultimate bearing capacity of concrete-filled steel tube can be improved by adding steel fiber and self-stress. Zhang et al. [18] conducted an axial compression test on high-strength microexpansive concrete-filled steel tubes, which showed that the bearing capacity of high-strength microexpansive concrete confined by steel tubes was higher than that of ordinary concrete confined by steel tubes, but the ductility was not significantly different. Huang et al. [19] believed that in the elastic stage, the bearing capacity of self-stressing microexpansive concrete-filled steel tube is 5%–20% higher than that of ordinary steel tube microexpansive concrete.

Domestic and foreign scholars mainly focus on the bearing capacity of self-stressing concrete-filled steel tubular columns, and there is little analysis on the influencing factors of self-stress of microexpansive concrete. As a result, this study carried out the experimental study of five steel tube-confined microexpansive concrete short columns and analyzed impactions that caused steel tube thickness, end constraint, expansion rate, section form, length-to-diameter ratio, and other parameters to the self-stress of microexpansive concrete, providing a reference for the application of steel tube-confined microexpansive concrete column in protection engineering.

## 2. Experimental Programs

**2.1. Specimen Design.** The expansion rate test of microexpansive concrete confined by a high-strength steel tube was carried out with different expansion rates of 8% and 12%. Then, five high-strength steel tube-confined microexpansive concrete (HSTCMC) short columns with dimensions of 159 mm (diameter)  $\times$  400 mm (height), and 168 mm (diameter)  $\times$  400 mm (height) were tested to explore the influence of microexpansive concrete self-stress on the mechanical performance of HSTCMC short columns. Specimen CS1 is the experimental control group, and specimens CS2 and CS3 mainly analyze the influence of different expansion rates on

the HSTCMC short columns. Specimens SC4 and SC5 mainly analyze the influence of steel tube diameter, thickness, and expansion rate on the HSTCMC short columns and further verify the reliability of the numerical calculation method and the accuracy of relevant parameters of the volume expansion model in finite element calculation. The detailed parameters of the specimens are shown in Table 1.

**2.2. Test Setup.** The volume expansion test device of microexpansive concrete confined by a high-strength steel tube is shown in Figure 1. After pouring and vibrating, the upper surface of the test specimen was scraped with a spatula and then sealed with the plastic film to reduce water loss of the microexpansion concrete. The specimen was placed vertically on the test bench, and the LR-30 laser displacement sensor was installed at the center of the top section to measure the vertical volume expansion of microexpansive concrete. When erecting the LR-30 laser displacement sensor, the instrument should be placed in a vertical state, to make sure that the laser axis emitted is parallel to the axis of the specimen. All data were automatically recorded by the DH3816-type dynamic data acquisition instrument, and the measurement period is 28 days.

To explore the influence of microexpansive concrete self-stress on the mechanical performance of HSTCMC short columns and verify the accuracy of the finite element model, the uniaxial compression test of the five specimens was carried out in the Laboratory of Structure and Bridge Engineering at the Nanjing University of Technology. The loading process was introduced as follows: (1) before the uniaxial compression test, a layer of fine sand was placed on the upper surface of the specimens to ensure that the steel tube and the microexpansive concrete are on the same horizontal plane to simultaneously share the load. (2) As shown in Figure 2, the displacement meters were, respectively, placed between the upper and lower loading plates to monitor the vertical deformation of the test specimens. The center of the HSTCMC short columns was aligned with the loading center of the servo-hydraulic testing machine by the preloading test so as to ensure that the specimen was under axial compression rather than eccentric compression. (3) The test devices were debugged, and the preloading test was started using the displacement control method of 2 mm/s, where the loading amplitude was 1,000 kN in this state and the duration was two minutes. (4) The formal loading test was begun with 2 mm/s, and the surface change of the HSTCMC short columns was monitored using a camera. When the vertical displacement of the test specimen is up to 100 mm or has a tendency to destabilize, the loading should be stopped and the test should be finished.

**2.3. Material Properties.** The design strength grade of the microexpansive concrete was C80, which was mixed together in a certain proportion from the P. O 52.5 ordinary Portland cement, the graded crushed stone (particle size 5–25 mm), river sand, silica fume, microbead, expansive agent, water, and water-reducing agent. The mix proportion of the microexpansive concrete is shown in Table 2. During

TABLE 1: Details of the specimens.

ID	Diameter (mm)	Height (mm)	Thickness (mm)	Concrete strength (MPa)	Volume expansion (%)	Length/diameter ( $L/d$ )
CS1	168	400	4	80	0	2.38
CS2	168	400	4	80	8%	2.38
CS3	168	400	4	80	12%	2.38
CS4	159	400	4	80	12%	2.51
CS5	159	400	3	80	12%	2.51

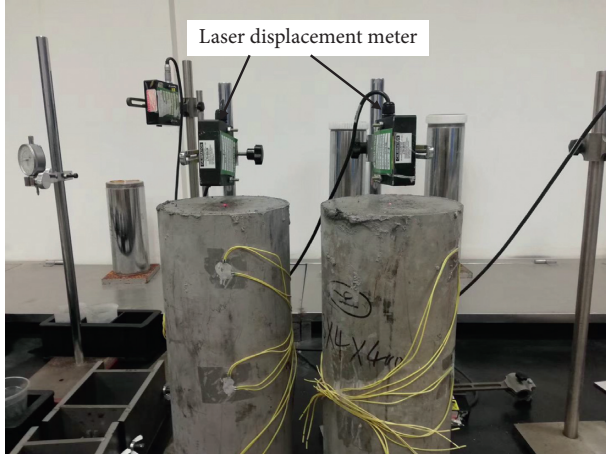


FIGURE 1: Axial free expansion test device.

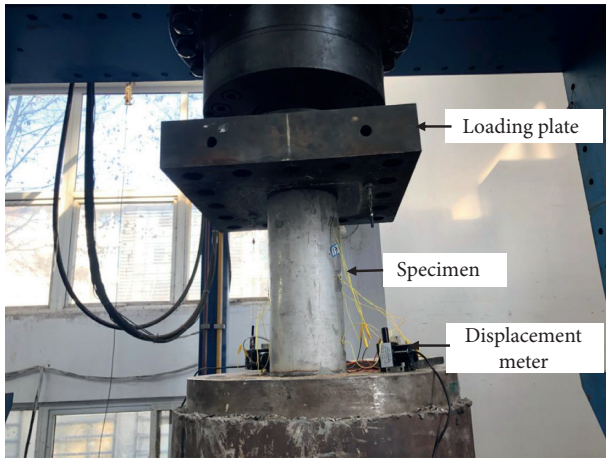


FIGURE 2: Loading device.

the pouring process of the test specimens, three micro-expansive concrete cube specimens with dimensions of  $150\text{ mm} \times 150\text{ mm} \times 150\text{ mm}$  were reserved according to the standard of “test methods for mechanical properties of ordinary concrete” (GB/T 50081–2016). After 28 days of indoor curing, the average compressive strength of the cube specimens for 28 days was 85 MPa. It should be noted that the steel tube used in the test is made of stainless steel. According to the standard of “metallic material tensile test method at ambient temperature” (GB/T 228.1–2010), the elastic modulus and uniaxial tensile strength of the steel tube are 208 GPa and 230 MPa, respectively.

### 3. Results and Discussion

**3.1. Test Results of the Free Expansion.** The relationship between the free expansion rate and age of different expansive agent contents is shown in Figure 3. In the initial stage, the expansion rate of the microexpansive concrete is growing faster, it reaches the peak value on the third day, and then, the expansion effect decreases continuously due to the shrinkage of the microexpansive concrete. When the expansion effect is less than the shrinkage effect of concrete, the drop segment appears in the cure, and the later curve is basically stable. The whole expansion process of concrete can be divided into three stages, namely, expansion stage, shrinkage stage, and stable stage. The reason is that before stabilization, the expansion energy generated by the concrete expansive agent is greater than the shrinkage energy, and then, the expansion energy gradually decreases in the process of expansion. When the expansion energy is less than the contraction energy, the shrinkage phenomenon appears and finally tends to be stable.

#### 3.2. Test Results

**3.2.1. Failure Mode.** As shown in Figure 4, the failure modes of all the HSTCMC short columns are drum shaped in the middle section and concave at the upper and lower ends. At the beginning of the loading test, there is no obvious deformation along the radial direction of the test specimen due to the specimens in the elastic deformation stage. With the increase in vertical load, the deformation of microexpansive concrete in the high-strength steel tube gradually increases. At the same time, the constraint effect of high-strength steel tube on microexpansive concrete is also increasing. The middle of the specimen begins to appear in drum state, and the two ends are in a concave state. From yielding to unloading, the specimens show good ductility.

The main failure form of the finite element results was the drum-bending failure of the high-strength steel tube, and there is no depression at both ends. The main reason was that the microexpansive concrete has certain material defects (such as pores) and the stress concentration at both ends in the test, while the whole microexpansive concrete was regarded as homogeneous material in the finite element analysis. Therefore, there was no depression at both ends of the specimen.

TABLE 2: Mix design of microexpansive concrete (kg).

ID	Cement	Silica fume	Mineral powder	Microbead	Expansive agent	Sand	Big stone	Small stone	Water	Water-reducing agent	$f_c$
$M_0$	16.5	0.89	1.08	1.91	—	22.7	23.93	10.25	6.19	0.12	83.6
$M_8$	12.6	0.75	0.92	1.62	1.38	19.3	20.30	8.70	4.03	0.07	85.2
$M_{12}$	11.9	0.75	0.92	1.62	2.08	19.3	20.36	8.70	4.03	0.07	86.2

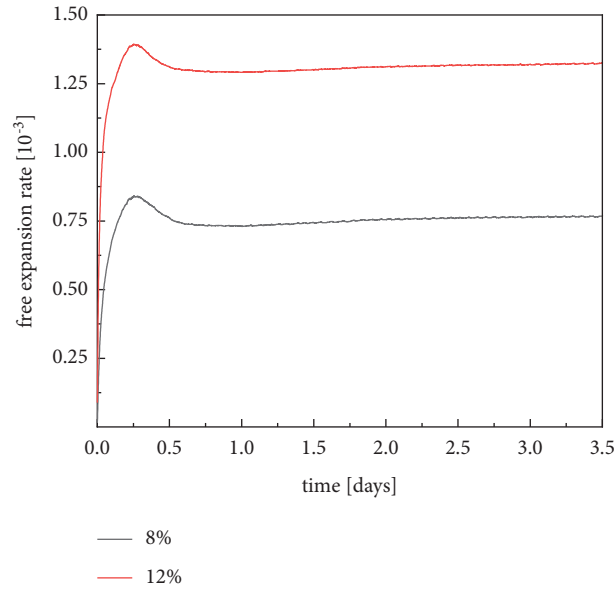


FIGURE 3: Free expansion-age curve.



FIGURE 4: Failure mode of the specimen. (a) Experimental result and (b) FE result.

**3.2.2. Stress-Strain Curve of the Test Specimens.** The mesh size of the sample has a great influence on the numerical simulation results. In order to analyze the sensitivity of numerical simulation results of grid size, this study takes sample C-1 as an example to analyze the influence of grid size on the results under the same boundary conditions and loading conditions. Figure 5 shows the load-displacement curves of specimens with different grid sizes. Compared with the test results, it can be seen from Figure 5 that when the grid size is 3 mm, 5 mm, and 8 mm, the ratio of the finite element to test in the load-displacement curve is basically

unchanged. Considering the calculation accuracy and efficiency, 8 mm mesh is selected for finite element analysis in this study.

As it can be seen from Figures 6 and 7, the yield strength of the HSTCMC short column is significantly higher than that of the ordinary concrete-filled steel tube. The yield strength of the HSTCMC short column added with 8% and 12% expansive agent were, respectively, increased by 8.9% and 14.9% compared to the control group (ordinary concrete-filled steel tube short column), indicating that the microexpansive concrete can greatly improve the load-

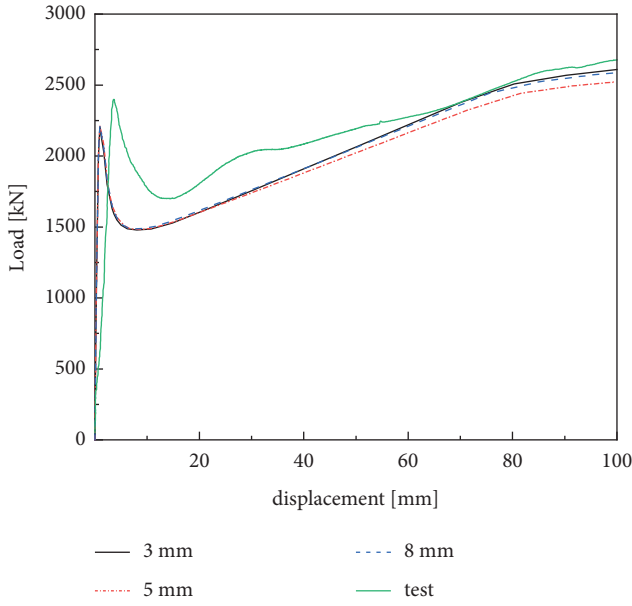


FIGURE 5: Load-displacement curves under different grid sizes.

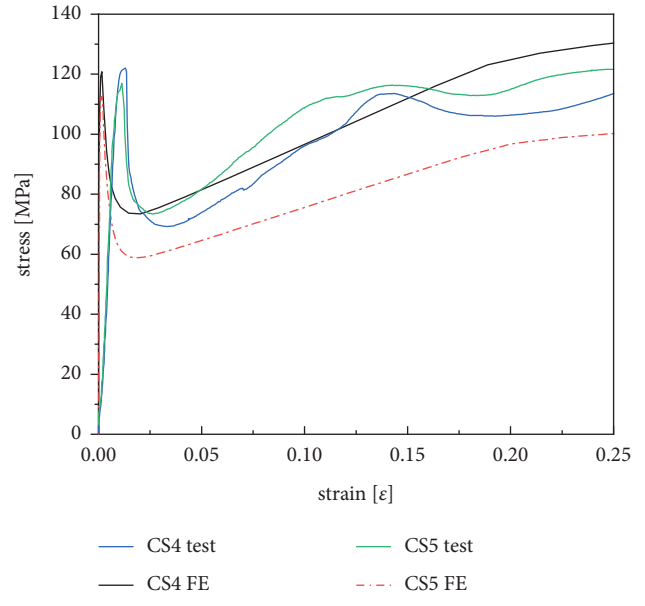


FIGURE 7: Stress-strain curves of different wall thicknesses.

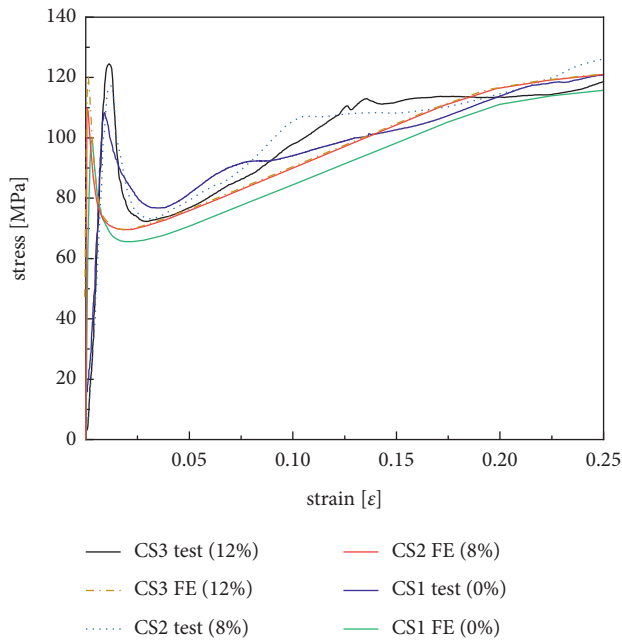


FIGURE 6: Stress-strain curves of different expansive.

bearing capacity of the HSTCMC short column. The reason is that the microexpansive concrete plays a positive role in compensating the shrinkage defects of ordinary concrete, and the self-stress can be generated under the dual action of concrete microexpansive and the high-strength steel tube constraint after the microexpansive concrete curing.

As shown in Figures 6 and 7, the change trends of the experimental results and FE results are almost the same. As shown in Table 3, the error of yield strength for the HSTCMC short column between the experimental results and the finite element simulation is 8.3%. Compared with the control group CS1, the yield strength of specimens CS2

and CS3 was improved by 6.8% and 2.8%, respectively, with the expansive agent ratio that increased from 8% to 12%. This is because the concrete self-stress was enhanced after increasing the expansive agent ratio.

The maximum displacement of the HSTCMC short column with 8% and 12% expansive agent is 0.336 mm and 0.557 mm, respectively, along the axis. With the content of the expansive agent that increased from 0% to 12%, the axial displacement of the HSTCMC short column increased by 39.7% compared to the control group. It shows that the expansion effect of different expansive agent content on concrete is different, and the stress state caused by different expansive agent content is not the same.

#### 4. Finite Element Analysis

**4.1. Establishment of FE Model.** The finite element model of the HSTCMC short column was established using the ABAQUS software to investigate the influence of microexpansive concrete on the mechanical performance of the HSTCMC short column. As shown in Figure 8, the high-strength steel tube was simulated by an eight-node linear hexahedron (C3D8R) element, and the constitutive model was a bilinear model. The  $\epsilon_1$  and  $\epsilon_2$  are the yield strain and ultimate strain, respectively, corresponding to the yield stress and ultimate stress of  $\sigma_1$  and  $\sigma_2$ ,  $E$  is the elastic modulus, and  $K$  is the tangent modulus of the high-strength steel tube after yielding. In this study, the elastic modulus of high-strength steel tube is 210 GPa, the Poisson's ratio is 0.28, and the yield strength is 230 MPa. As shown in Figure 7(b), the microexpansive concrete with C80 strength grade adopts the model recommended by Guo [20]. The elastic modulus is 45 GPa, Poisson's ratio is 0.2, and the 28-d compressive strength is 85 MPa.

In the finite element model, the lower and top steel plate and the steel tube are restrained together using the tie

TABLE 3: Feature parameters of key points.

Specimen	Yield load (MPa)		Test/FE value	Yield displacement (mm)		Test/FE value
	Test results	FE results		Test results	FE results	
CS1	2399	2199	1.09	3.59	1.29	2.78
CS2	2612	2434	1.07	4.8	0.9	5.33
CS3	2749	2672	1.03	4.77	0.6	7.95
CS4	2422	2397	1.01	5.24	0.64	8.18
CS5	2275	2247	1.03	4.13	0.65	6.35
Average			1.046			6.11
Deviation			0.001			4.856

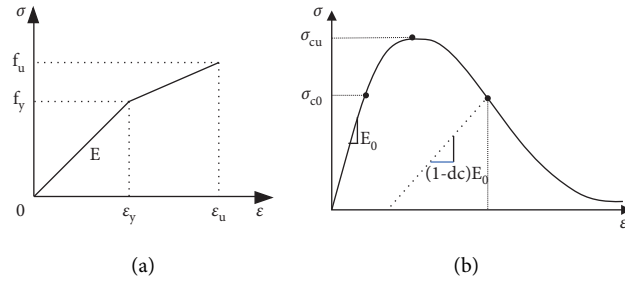


FIGURE 8: Stress-strain relationship of the materials. (a) Steel tube and (b) microexpansive concrete.

constraint of the software. The inside surface of the steel tube and the core microexpansive concrete are connected with each other by the penalty function, in which the friction coefficient of the bonding surface is 0.6, and the normal contact is the linear relationship with the contact stiffness of 45 GPa (equal to the elastic modulus of concrete). As shown in Figure 9, the bottom surface of the HSTCMC short column was set as a completely fixed boundary, that is,  $U_x = U_y = U_z = UR_x = UR_y = UR_z = 0$ , and on the top of the test piece, it has no special treatment. The vertical load is realized by the displacement control method. In addition, the thermal expansion principle is used to simulate the self-stress process of the microexpansive concrete in the FE model. The linear expansion coefficient of the microexpansive concrete is  $10 \times 10^{-6}/^\circ\text{C}$  for vertical direction and  $10 \times 10^{-5}/^\circ\text{C}$  for radial direction, respectively [21], which were validated in the following paragraph.

The free expansion rate at  $42^\circ\text{C}$  and  $50^\circ\text{C}$  was obtained by finite element analysis. The function of the finite element model at different temperatures was obtained by fitting the two curves. The fitting formula is shown in Figure 10. Using the test results of free expansion data as a reference, when the temperature of concrete increases by  $45^\circ\text{C}$ , the concrete expands 0.554 mm along the axis, which is only 0.003 mm different from the experimental results with 12% expansive agent, and the error is only 0.5%. In the same way, using the temperature fitting formula of Figure 10 when the concrete temperature is increased by  $27^\circ\text{C}$  to simulate the experiment of adding 8% expansive agent, the difference between the experimental results is only 0.9%. The experimental results and finite element results are shown in Figure 11. Clearly, the finite element results are in good agreement with the experimental results, which can be used to simulate the volume expansion of microexpansive concrete confined by the high-strength steel tube.

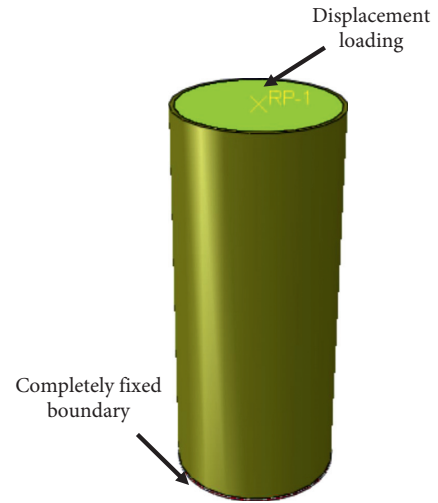


FIGURE 9: Boundary condition.

Figure 12 shows the comparison of the test and finite element simulation results for the test specimens CS1, CS2, and CS3, and the change trends of the experimental results and FE results are almost the same. As shown in Table 3, it can be seen that the yield strength of the numerical simulation results is less than the test calculation results, and the errors between them are within 10%. That is, the finite element results are in good agreement with the test results.

**4.2. Parameter Analysis.** In this study, the maximum stress is selected for analysis (regardless of direction). From the finite element results in Figure 13, it can be concluded that the maximum axial stress (S33) of concrete is 5.68 MPa, which appears at the top of concrete, and the maximum

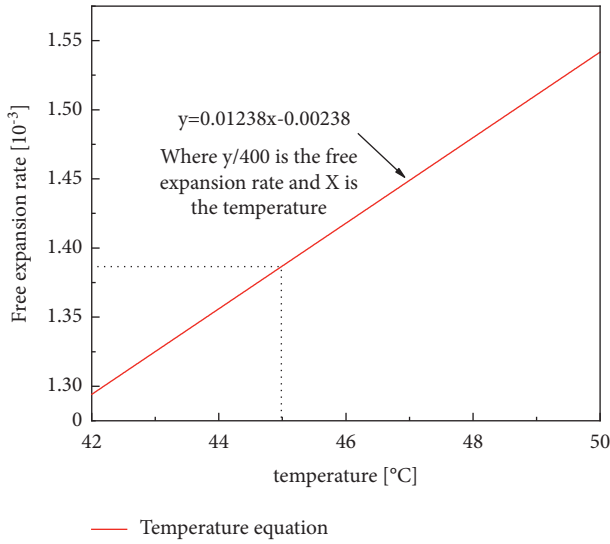


FIGURE 10: Comparison of test results and FE results.

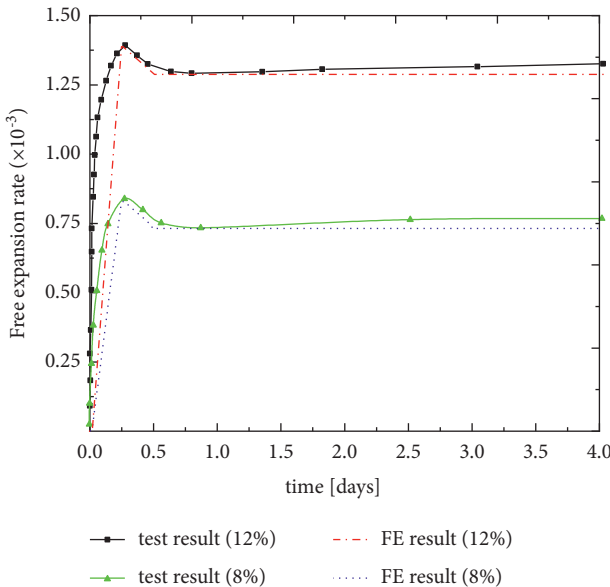


FIGURE 11: Temperature equation curve.

circumferential stress ( $S_{12}$ ) is 3.91 MPa. It appears at the bottom of the concrete, so the parameter analysis of the stress change trend is carried out at the same position as the sample.

As shown in Figures 14–18, the left side of the  $y$ -axis represents the axial stress of microexpansive concrete, the right side of the  $y$ -axis represents the hoop stress of microexpansive concrete, and the  $y$ -axis represents the self-stress values of microexpansive concrete. It should be noted that the tension stress is positive, and the compression stress is negative. As shown in Figure 14 that the axial stress and hoop stress of the microexpansive concrete can be effectively enhanced by increasing the content of the expansive agent, the hoop stress of the microexpansive concrete is relatively larger than the axial stress. This is due to the specimen is freely expandable in the axial direction, and the steel tube is

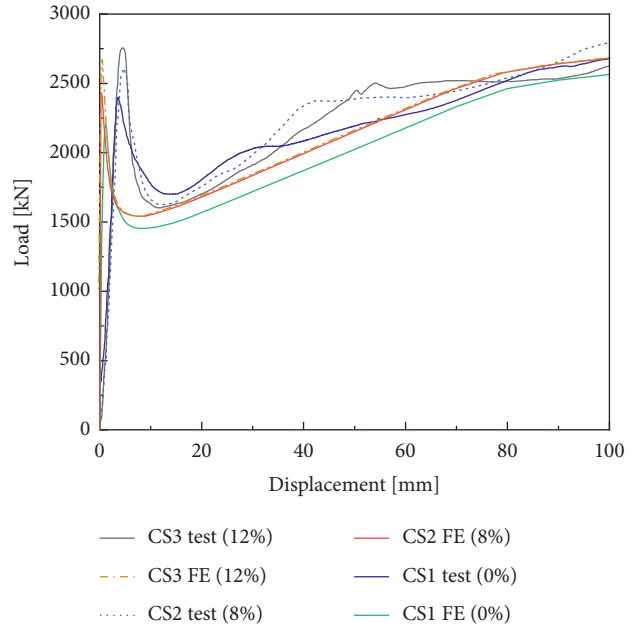


FIGURE 12: Load-displacement curve of the specimen.

constrained in the hoop direction. Under the three-dimensional constraint of the steel tube, the hoop stress of the microexpansive concrete is larger than the axial stress.

As shown in Figure 15, the hoop stress of the microexpansive concrete increases by 43% with the thickness of the high-strength steel tube that increased from 4 mm to 8 mm. The main reason is that the thickness of the steel tube increases the three-dimensional constraint of the steel tube on the microexpansive concrete, so the self-stress of the microexpansive concrete increases greater. However, with the increase in the thickness of the high-strength steel tube, the increase range of stress decreases, which may be because the steel tube can only increase the self-stress of microexpansive concrete within a certain range of thickness. The axial stress decreases gradually with the increase in the thickness of the steel tube. The main reason may be that the interaction friction force between the steel tube and the microexpansive concrete increased in the axial direction due to the increase in the self-stress of microexpansive concrete.

The specimen with a square cross section is prone to stress concentration at the corner. It can be seen from Figure 16 that the hoop stress and axial stress produced by microexpansive concrete are greater than those of the circular section at the corner position. In the noncorner position, the hoop stress and axial stress produced by microexpansive concrete are less than those of the circular section. The reason is that the sidewall of the high-strength steel tube for the square cross section will deform together with the microexpansive concrete during the volume expansion process and then completely confine the core concrete. That is, the constraint effect of the circular cross section is superior to that of the square cross section.

As shown in Figure 17 that the hoop stress of axial limited expansion (with 3 mm steel plate at both ends of the specimen) is larger than that of the axial unlimited

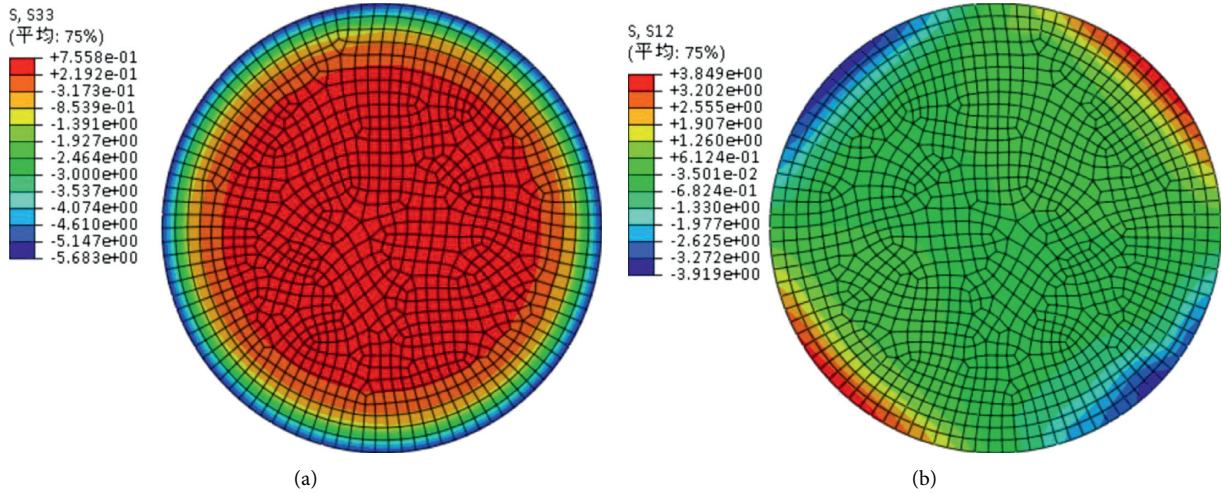


FIGURE 13: Hoop (S12) and axial stress (S33) distribution.

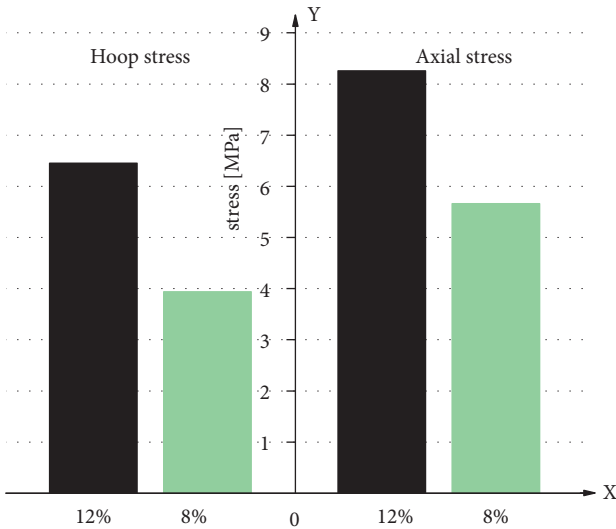


FIGURE 14: Stress of different expansive agents.

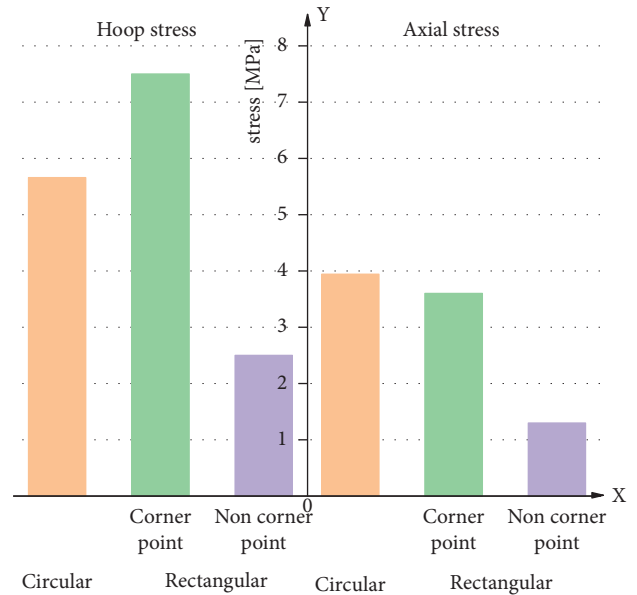


FIGURE 16: Stress of different section forms.

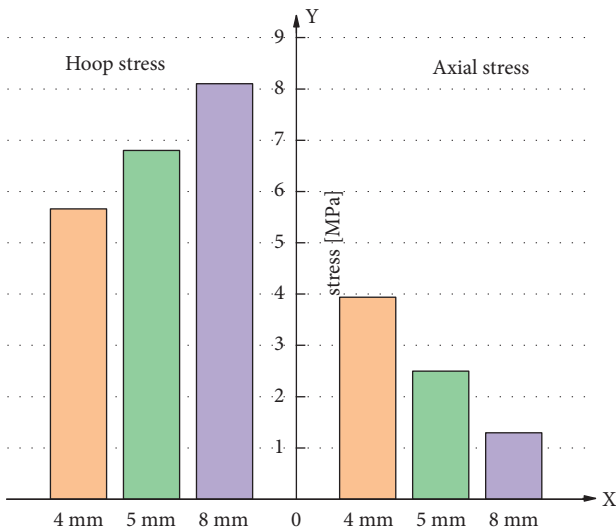


FIGURE 15: Stress of different wall thicknesses.

expansion (one end with 3 mm steel plate and the other end is not restricted expansion). This is because the axial expansion of the microexpansive concrete is limited by the two steel plates at both ends, so the microexpansive concrete is in the axial compression state.

It can be seen from Figure 18 that both the axial stress and hoop stress of the microexpansive concrete were decreased with the length-to-diameter ratio that increased from 2.38 to 3.57. The main reason is that the length of the short column of the microexpansion concrete-filled steel tube is increased, caused by the slow expansion of the specimen, and the axial stress will be reduced due to the increase in gravity. The influence of microexpansive concrete self-stress on the performance of the HSTCMC short column ( $L/D \leq 4$ ) was studied in this study. However, the effect of self-stress of microexpansive concrete on the medium and long HSTCMC column needs to be further verified.



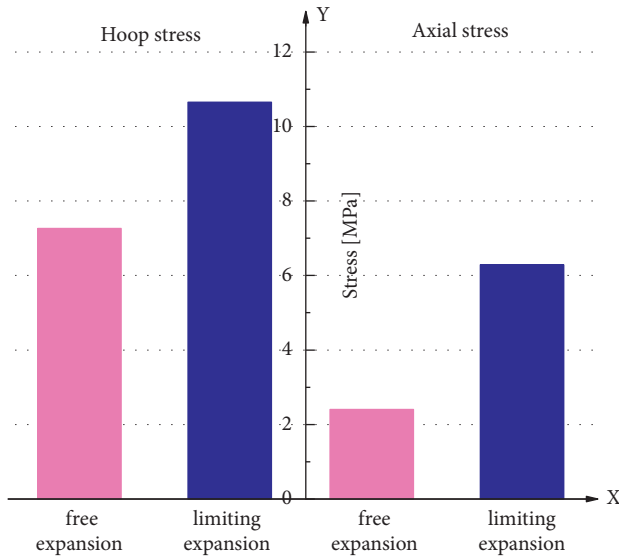


FIGURE 17: Stress of free expansion and limited expansion.

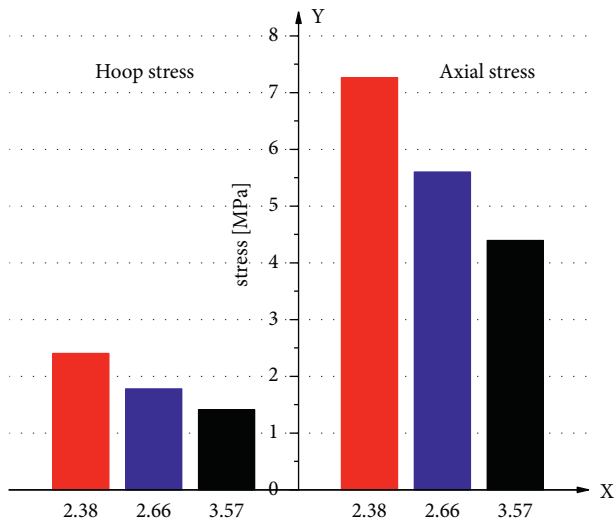


FIGURE 18: Self-stress of microexpansive concrete for different length-to-diameter ratio.

## 5. Conclusions

To explore the influence of microexpansive concrete self-stress on the performance of steel pipe concrete, the expansion rate test of microexpansive concrete confined by steel tube was carried out with different expansion rates. Then, the mechanical properties of high-strength steel tube confine microexpansive concrete (HSTCMC) short columns were conducted by the uniaxial compression test. Furthermore, the ABAQUS software was employed to analyze the microexpansive mechanism of the concrete, and it was verified by the uniaxial compression test; the following conclusions can be drawn:

- (1) The microexpansive concrete can greatly induce the shrinkage phenomenon of ordinary concrete, in which volume expansion can be up to  $150 \mu\epsilon$  after

four days of maintenance time. The axial stress and hoop stress of the microexpansive concrete can be effectively enhanced by increasing the content of the expansive agent, and the hoop stress of the microexpansive concrete is relatively larger than the axial stress.

- (2) The mechanical performance of the HSTCMC short columns can be greatly improved after using microexpansive concrete instead of normal concrete. The yield strength of the HSTCMC short columns was increased by 14.6% compared to the control group, and the corresponding displacements were 3.59 mm and 4.77 mm.
- (3) The hoop stress of the microexpansive concrete was increased by 43% with the thickness of the high-strength steel tube that increased from 4 mm to 8 mm. The hoop stress and axial stress produced by microexpansive concrete are greater than those of the circular section at the corner position. In the noncorner position, the hoop stress and axial stress produced by microexpansive concrete are less than those of the circular section.
- (4) For the HSTCMC short column, both the axial stress and hoop stress of the microexpansive concrete were decreased with the length-to-diameter ratio that increased from 2.38 to 3.57.

## Data Availability

The datasets generated and analyzed during the current study are available from the corresponding author upon reasonable request.

## Conflicts of Interest

The authors declare that they have no conflicts of interest.

## Acknowledgments

The authors gratefully acknowledge the financial support provided by the National Natural Science Foundations of China (no. 51738011) and the Postdoctoral Fund of Jiangsu Province (no. 2018K087B).

## References

- [1] E. M. Güneyisi and A. I. Nour, "Axial compression capacity of circular CFST columns transversely strengthened by FRP," *Engineering Structures*, vol. 191, no. 1, pp. 417–431, 2019.
- [2] J.-B. Yan, X. Dong, and T. Wang, "Axial compressive behaviours of square CFST stub columns at low temperatures," *Journal of Constructional Steel Research*, vol. 164, no. 1, Article ID 105812, 2020.
- [3] L. He, Y. Zhao, and S. Lin, "Experimental study on axially compressed circular CFST columns with improved confinement effect," *Journal of Constructional Steel Research*, vol. 140, pp. 74–81, 2018.
- [4] H. Dong, Y. Li, W. Cao, Q. Qiao, and R. Li, "Uniaxial compression performance of rectangular CFST columns with

- different internal construction characteristics,” *Engineering Structures*, vol. 176, pp. 763–775, 2018.
- [5] Y. H. Huang, A. R. Liu, J. Y. Fu, and Y. L. Pi, “Experimental investigation of the flexural behavior of CFST trusses with interfacial imperfection,” *Journal of Constructional Steel Research*, vol. 137, no. 10, pp. 52–65, 2017.
- [6] Y. Ouyang and A. K. H. Kwan, “Finite element analysis of square concrete-filled steel tube (CFST) columns under axial compressive load,” *Engineering Structures*, vol. 156, pp. 443–459, 2018.
- [7] S. G. Huang and L. Yue, “Research on the hydration, hardening mechanism, and microstructure of high-performance expansive concrete,” *Cement and Concrete Research*, vol. 29, no. 7, pp. 1013–1017, 1999.
- [8] L. Xu, P. Zhou, Y. Chi, L. Huang, J. Ye, and M. Yu, “Performance of the high-strength self-stressing and self-compacting concrete-filled steel tube columns subjected to the uniaxial compression,” *International Journal of Civil Engineering*, vol. 16, no. 9, pp. 1069–1083, 2018.
- [9] L. H. Xu, F. Z. Xu, and P. H. Zhou, “Experimental study on compression behavior of steel tube self-stressing and self-compacting high strength micro expansive concrete medium long columns,” *Journal of Civil Engineering*, vol. 049, no. 011, pp. 26–34, 2016, In Chinese.
- [10] N. Li, Y. Lu, S. Li, and D. Gao, “Axial compressive behaviour of steel fibre reinforced self-stressing and self-compacting concrete-filled steel tube columns,” *Engineering Structures*, vol. 222, Article ID 111108, 2020.
- [11] B. Wang, J. Zhao, and Q. Wang, “Distributed models of self-stress value in textile-reinforced self-stressing concrete,” *Construction and Building Materials*, vol. 126, pp. 286–296, 2016.
- [12] Y. Y. Lu, B. Yan, N. Li, and S. Li, “Compressive behavior of steel tube columns filled with steel fiber reinforced self-stressing and self-compacting concrete,” *Journal of Civil Engineering and Management*, vol. 034, no. 2, pp. 1–4, 2017, in Chinese.
- [13] Y. Y. Lu, Z. Z. Liu, S. Li, and N. Li, “Bond behavior of steel fibers reinforced self-stressing and self-compacting concrete filled steel tube columns,” *Construction and Building Materials*, vol. 158, pp. 639–651, 2018.
- [14] F. He, X. H. Zhou, and C. H. Tang, “Experimental study on bearing capacity of high strength micro expansive concrete filled steel tubular short columns under axial compression,” *Engineering Mechanics*, vol. 17, no. 4, pp. 61–66, 2000, in Chinese.
- [15] Y.-y. Lu, N. Li, S. Li, and H.-j. Liang, “Experimental investigation of axially loaded steel fiber reinforced high strength concrete-filled steel tube columns,” *Journal of Central South University*, vol. 22, no. 6, pp. 2287–2296, 2015.
- [16] Z. Liu, Y. Lu, S. Li, and S. Yi, “Behavior of steel tube columns filled with steel-fiber-reinforced self-stressing recycled aggregate concrete under axial compression,” *Thin-Walled Structures*, vol. 149, pp. 2287–2296, Article ID 106521, 2020.
- [17] S. M. Zhang, J. P. Liu, and L. Ma, “Experimental study and bearing capacity analysis of high strength micro expansive concrete short columns confined by circular steel tubes,” *Journal of Civil Engineering*, vol. 40, no. 3, pp. 24–31, 2007, in Chinese.
- [18] C. K. Huang, L. Xu, and Y. Liu, “Experimental study on mechanical properties of self-compacting and self-stressing concrete filled steel tubular stub columns under axial compression,” *Journal of Dalian University of technology*, vol. 46, no. 5, pp. 77–82, 2006, in Chinese.
- [19] H. Wei, Z. C. Fan, P. L. Shen, and N. Lu, “Experimental and numerical study on the compressive behavior of micro-expansive ultra-high-performance concrete-filled steel tube columns,” *Construction and Building Materials*, vol. 254, Article ID 119150, 2020.
- [20] Z. H. Guo, *Principles of Reinforced concrete*, Tsinghua University Press, Beijing, China, 2015, in Chinese.
- [21] S. Wang, *Experiment and Numerical Simulation of Linear Expansion Coefficient of Rockfill concrete*, Tsinghua University, Beijing, China, 2012, in Chinese.